J|A|C|S
ARTICLES
Published on Web 03/20/2003

Biosynthesis of Riboflavin. Single Turnover Kinetic Analysis of 6,7-Dimethyl-8-ribityllumazine Synthase*

Nicholas Schramek, Ilka Haase, Markus Fischer, and Adelbert Bacher*

Contribution from the Lehrstuhl für Organische Chemie und Biochemie, Technische Universität München, Lichtenbergstr. 4, D-85747 Garching, Germany

Received August 21, 2002; E-mail: adelbert.bacher@ch.tum.de

Abstract: 6,7-Dimethyl-8-ribityllumazine synthase (lumazine synthase) catalyzes the condensation of 5-amino-6-ribitylamino-2,4-(1*H*,3*H*)-pyrimidinedione with 3,4-dihydroxy-2-butanone 4-phosphate, affording the riboflavin precursor, 6,7-dimethyl-8-ribityllumazine. Single turnover experiments monitored by multi-wavelength photometry were performed with the recombinant lumazine synthase of *Bacillus subtilis*. Mixing of the enzyme with the pyrimidine type substrate is conducive to a hypsochromic shift as well as a decrease in absorbance of the heterocyclic substrate; the rate constant for that reaction is 0.02 s^{-1} μM^{-1}. Rapid mixing of the complex between enzyme and pyrimidine type substrate with the second substrate, 3,4-dihydroxy-2-butanone 4-phosphate, is followed by the appearance of an early optical transient characterized by an absorption maxima at 330 nm of low intensity which was tentatively assigned as a Schiff base intermediate. The subsequent elimination of phosphate affords a transient with intense absorption maxima at 455 and 282 nm, suggesting an intermediate with an extended system of conjugated double bonds. The subsequent formation of the enzyme product, 6,7-dimethyl-8-ribityllumazine, is the rate-determining step.

Introduction

Flavocoenzymes derived from vitamin B_2 (riboflavin) are essential for the metabolism of all organisms. The vitamin is biosynthesized in plants and numerous microorganisms, whereas animals are absolutely dependent on nutritional sources.

The biosynthetic pathway conducive to riboflavin has been studied in some detail.[1−3] Briefly, GTP is converted to 5-amino-6-ribitylamino-2,4-(1*H*,3*H*)-pyrimidinedione (compound **2**, Figure 1) which is then condensed with the carbohydrate 3,4-dihydroxy-2-butanone 4-phosphate (compound **1**, Figure 1), affording 6,7-dimethyl-8-ribityllumazine (compound **8**) under the catalytic action of 6,7-dimethyl-8-ribityllumazine synthase (lumazine synthase).[4] The pteridine derivative undergoes an unusual dismutation, affording riboflavin and 5-amino-6-ribitylamino-2,4-(1*H*,3*H*)-pyrimidinedione (compound **2**) which is catalyzed by riboflavin synthase. The pyrimidine derivative **2** is reutilized as substrate by lumazine synthase. In summary, 1 equiv. of riboflavin is formed from 1 equiv. of the pyrimidine derivative **2** and 2 equiv. of the carbohydrate **1**.[5]

Structures of lumazine synthases from microorganisms and plants have been studied by X-ray crystallography. The enzymes from fungi and from the bacterium *Brucella abortus* are homopentamers.[6−9] Lumazine synthases from a variety of other bacteria and from plants are icosahedral capsids of 60 identical subunits which are best described as dodecamers of pentamers.[6,10−12]

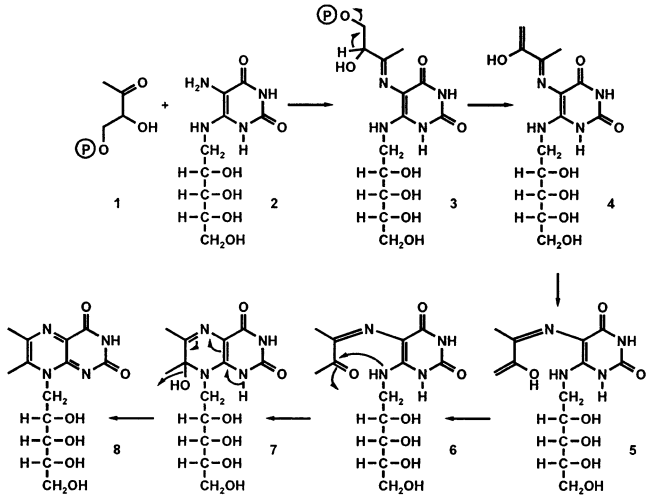

Figure 1. Hypothetical reaction mechanism for 6,7-dimethyl-8-ribityllumazine synthase.[4]

* Corresponding author.

(1) Bacher, A.; Eberhardt, S.; Eisenreich, W.; Fischer, M.; Herz, S.; Illarionov, B.; Kis, K.; Richter, G. *Vitam. Horm.* **2001**, *61*, 1−49.
(2) Young, D. W. *Nat. Prod. Rep.* **1986**, *3*, 395−419.
(3) Bacher, A.; Eberhardt, S.; Richter, G. In *Escherichia coli and Salmonella typhimurium*, 2nd ed.; Neidhardt, F. C., Ingraham, J. L., Low, K. B., Magasanik, B., Schaechter, M., Umbarger, H. E., Eds.; American Society for Microbiology: Washington, D.C., 1996; Vol. 1, pp 657−664.
(4) Kis, K.; Volk, R.; Bacher, A. *Biochemistry* **1995**, *34*, 2883−2892.
(5) Plaut, G. W. *J. Biol. Chem.* **1960**, *235*, PC41−42.
(6) Persson, K.; Schneider, G.; Jordan, D. B.; Viitanen, P. V.; Sandalova, T. *Protein Sci.* **1999**, *8*, 2355−2365.
(7) Braden, B. C.; Velikovsky, C. A.; Cauerhff, A. A.; Polikarpov, I.; Goldbaum, F. A. *J. Mol. Biol.* **2000**, *297*, 1031−1036.
(8) Meining, W.; Mörtl, S.; Fischer, M.; Cushman, M.; Bacher, A.; Ladenstein, R. *J. Mol. Biol.* **2000**, *299*, 181−197.
(9) Gerhardt, S.; Haase, I.; Steinbacher, S.; Kaiser, J. T.; Cushman, M.; Bacher, A.; Huber, R.; Fischer, M. *J. Mol. Biol.* **2002**, *318*, 1317−1329.
(10) Ritsert, K.; Huber, R.; Turk, D.; Ladenstein, R.; Schmidt-Bäse, K.; Bacher, A. *J. Mol. Biol.* **1995**, *253*, 151−167.
(11) Zhang, X.; Meining, W.; Fischer, M.; Bacher, A.; Ladenstein, R. *J. Mol. Biol.* **2001**, *306*, 1099−1114.
(12) Ladenstein, R.; Schneider, M.; Huber, R.; Bartunik, H. D.; Wilson, K.; Schott, K.; Bacher, A. *J. Mol. Biol.* **1988**, *203*, 1045−1070.

10.1021/ja028226k CCC: $25.00

The peptide folds of pentameric and icosahedral lumazine synthase are closely similar. The active sites of all lumazine synthases are invariably located at subunit interfaces of the pentamer assemblies. The lumazine synthases of *Bacillaceae* contain a riboflavin synthase trimer in the core of the icosahedral capsid.[13−15] This complex topology is conducive to kinetic anomalies best described as substrate channeling.[16]

Certain pathogenic microorganisms such as *Enterobacteriaceae* are unable to absorb riboflavin or its derivatives from the environment and are therefore absolutely dependent on the endogenous synthesis of the vitamin.[17,18] Inhibitors of the riboflavin pathway could therefore serve as antiinfective agents. In light of the rapid resistance development, the exploration of novel antiinfective targets appears urgent, and information on the structure and mechanism of riboflavin biosynthetic enzymes could serve as a basis for their development. To elucidate the reaction mechanism of lumazine synthase, we have performed presteady-state kinetic experiments reported in this paper.

Experimental Procedures

Materials. 3,4-Dihydroxy-2-butanone 4-phosphate was prepared from ribose 5-phosphate using recombinant 3,4-dihydroxy-2-butanone synthase.[19] 5-Nitro-6-ribitylamino-2,4-(1*H*,3*H*)-pyrimidinedione[20] and 6,7-dimethyl-8-ribityllumazine[13] were synthesized according to published procedures. 5-Amino-6-ribitylamino-2,4-(1*H*,3*H*)-pyrimidinedione was freshly prepared as described earlier.[21]

Purification of Recombinant *B. subtilis* Lumazine Synthase. The recombinant *B. subtilis* strain BR151[pBL1]-p602-BS-ribH[22] was grown aerobically as described in LB medium containing 15 mg of erythromycin and 20 mg of kanamycin per liter at 32 °C. At an optical density of 0.7 (600 nm), isopropylthiogalactoside was added to a concentration of 2 mM. The suspension was incubated at 32 °C for 12 h, and the cells were harvested by centrifugation. Wet cell mass from 1 L of bacterial culture was suspended in 30 mL of 50 mM potassium phosphate, pH 7.0, containing 0.5 mM sodium sulfite, 0.5 mM EDTA, and 3 mg of lysozyme. The suspension was incubated for 20 min at 37 °C and was subsequently ultrasonically treated. The cells were centrifuged, and the supernatant was applied to a column of Q-Sepharose FF (3 × 25 cm) that had been equilibrated with 20 mM potassium phosphate, pH 7.0. The column was washed with 100 mL of 20 mM potassium phosphate, pH 7.0, and was subsequently developed with a gradient of 20−1000 mM potassium phosphate, pH 7.0 (total volume, 800 mL), at a flow rate of 2 mL min^{-1}. Fractions were combined and concentrated by ultracentrifugation (32 000 rpm, 16 h, 4 °C). The solution was applied to a Sephacryl 400 column (2.6 × 60 cm) that had been equilibrated with 100 mM potassium phosphate, pH 7.0. The column was developed with 500 mL of 100 mM potassium phosphate, pH 7.0, at a flow rate of 3 mL min^{-1}. Fractions were combined and concentrated by ultracentrifugation. The enzyme was stored at 4 °C in 100 mM potassium phosphate, pH 7.0.

Equilibrium Dialysis. Equilibrium dialysis experiments were performed as published elsewhere.[23]

Single Turnover Experiments. Stopped flow experiments were performed with an SFM4/QS apparatus from Bio-Logic (Claix, France) equipped with a linear array of three mixers and four independent syringes. The content of a 1.5 mm light path quartz cuvette behind the last mixer was monitored with a Tidas diode array spectrophotometer (200−610 nm) equipped with a 15 W deuterium lamp as light source (J&M Analytische Mess- und Regeltechnik, Aalen, Germany). The reaction buffer contained 100 mM potassium phosphate, pH 6.9, and 5 mM dithiotreithol. The enzyme and all substrates were diluted in reaction buffer. Solutions were mixed at 25 °C with a total flow rate of 4 mL s^{-1}. Optical spectra integrated over 96 ms were recorded at intervals of 100 ms in the wavelength range of 240−500 nm.

Data Analysis. Optical spectra were corrected for absorbance of buffer and enzyme by subtraction of a blank data set obtained without addition of substrate. Data reduction and stronger weighting of early spectra were achieved by extracting 300 spectra on a pseudo-logarithmic time base from the difference data sets. These data sets were then analyzed using the program SPECFIT/32 3.0.30 (Spectrum Software Associates, Marlborough, MA).

Determination of Reaction Order. Experiments were performedd by the initial rate method using the SFM4/QS apparatus described previously. The reaction buffer contained 100 mM potassium phosphate, pH 6.9, and 5 mM dithiotreithol. The enzyme and all substrates were diluted in reaction buffer. Solutions were mixed at 20 °C with a total flow rate of 4 mL s^{-1}. Absorbance at 284 nm was recorded over a period of 5 s at intervals of 10 ms. Enzyme and compound **2** were used in the concentration range of 20−200 μM.

Analytical Ultracentrifugation. Sedimentation velocity experiments were performed with an analytical ultracentrifuge (Optima XL-A, Beckman Instruments) equipped with absorbance and interference optics. Experiments were performed in double sector cells with aluminum centerpieces and sapphire windows. Protein concentration was monitored photometrically at 280 nm. Protein solutions were dialyzed against 50 mM potassium phosphate, pH 7.0.

Results

A hypothetical reaction mechanism of lumazine synthase is summarized in Figure 1.[16] Based on the known regiochemistry of the enzyme,[4,24] it has been suggested that the carbonyl group of 3,4-dihydroxy-2-butanone 4-phosphate (compound **1**) reacts with the position 5 amino group of the pyrimidine derivative **2** under formation of a Schiff base (compound **3**) which is assumed to eliminate inorganic phosphate under formation of compound **4**.[4,25] Tautomerization of compound **5** could afford the conjugated iminoketone **6**. Cyclization by addition of the position 8 ribitylamino group of compound **6** to the carbonyl group could yield a hydrated pteridin species, and dehydration could terminate the reaction.

Certain reactants involved in that hypothetical reaction sequence have characteristic visible and/or ultraviolet absorption. The substrate, **2**, has an absorption maximum at 284 nm at pH 7.0. Lumazine synthase binds compound **2** with an apparent K_D of about 9 μM. Notably, in a mixture with lumazine synthase, the absorbance of compound **2** is significantly lowered and shifted to 278 nm (Figure 2A).

The enzyme product, 6,7-dimethyl-8-ribityllumazine, has a highly characteristic spectrum with maxima at 408 and 255 nm

(13) Bacher, A. *Methods Enzymol.* **1986**, *122*, 192−199.
(14) Bacher, A.; Schnepple, H.; Mailänder, B.; Otto, M. K.; Ben-Shaul, Y. *Flavins Flavoproteins, Proc. Int. Symp., 6th* **1980**, 579−586.
(15) Ludwig, H. C.; Lottspeich, F.; Henschen, A.; Ladenstein, R.; Bacher, A. *Flavins Flavoproteins, Proc. Int. Symp., 8th* **1984**, 379−382.
(16) Kis, K.; Bacher, A. *J. Biol. Chem.* **1995**, *270*, 16788−16795.
(17) Lingens, F.; Oltmanns, O.; Bacher, A. *Z. Naturforsch., B: Chem. Sci.* **1967**, *22*, 755−758.
(18) Logvinenko, E. M.; Trach, V. M.; Koltun, L. V.; Shavlovskii, G. M. *Tr. S'ezda Mikrobiol. Ukr. 4th* **1975**, 8−9.
(19) Richter, G.; Krieger, C.; Volk, R.; Kis, K.; Ritz, H.; Götze, E.; Bacher, A. *Methods Enzymol.* **1997**, *280*, 374−382.
(20) Cresswell, R. M.; Wood, H. C. S. *J. Chem. Soc.* **1960**, 4768−4775.
(21) Bacher, A.; Baur, R.; Eggers, U.; Harders, H. D.; Otto, M. K.; Schnepple, H. *J. Biol. Chem.* **1980**, *255*, 632−637.
(22) Braun, N.; Tack, J.; Fischer, M.; Bacher, A.; Bachmann, L.; Weinkauf, S. *J. Cryst. Growth* **2000**, *212*, 270−282.
(23) Fischer, M.; Haase, I.; Feicht, R.; Richter, G.; Gerhardt, S.; Changeux, J. P.; Huber, R.; Bacher, A. *Eur. J. Biochem.* **2002**, *269*, 519−526.
(24) Nielsen, P.; Neuberger, G.; Fujii, I.; Bown, D. H.; Keller, P. J.; Floss, H. G.; Bacher, A. *J. Biol. Chem.* **1986**, *261*, 3661−3669.
(25) Volk, R.; Bacher, A. *J. Am. Chem. Soc.* **1988**, *110*, 3651−3653.

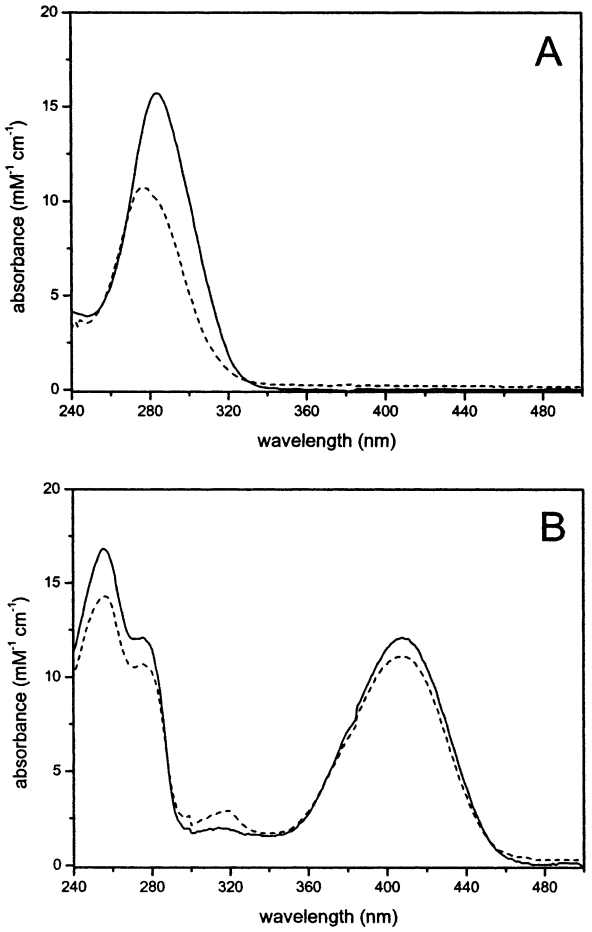

Figure 2. Ultraviolet spectra at pH 6.9. (A) (—) free 5-amino-6-ribitylamino-2,4-(1*H*,3*H*)-pyrimidinedione (compound **2**), (- - - -) enzyme bound 5-amino-6-ribitylamino-2,4-(1*H*,3*H*)-pyrimidinedione (compound **2**); (B) (—) free 6,7-dimethyl-8-ribityllumazine (compound **8**), (- - - -) enzyme bound 6,7-dimethyl-8-ribityllumazine (compound **8**).

and a shoulder at 276 nm at neutral pH (Figure 2B). The compound has a p*K* of about 8.3,[26] and deprotonation affords an equilibrium mixture of various anionic forms arising by intramolecular addition of alditol side chain hydroxy groups to ring carbon atom 7 under formation of various tricyclic structures with absorbance maxima at 313, 279, and 227 nm;[27,28] an exomethylene type anion species present in low amounts in the equilibrium mixture may absorb in the long wavelength range around 366 nm.[28]

Lumazine synthase of *B. subtilis* was purified using anionic exchange chromatography and gel filtration as described under Experimental Procedures. The protein showed a single 16 kDa band when analyzed by SDS polyacrylamide gel electrophoresis. Analytical gel permeation chromatography of the native protein afforded a single peak with the retention volume characteristic of the 60-mer. Analytical ultracentrifugation afforded a single, symmetrical boundary indicating an apparent sedimentation coefficient of 25 S in agreement with earlier studies.[21,29]

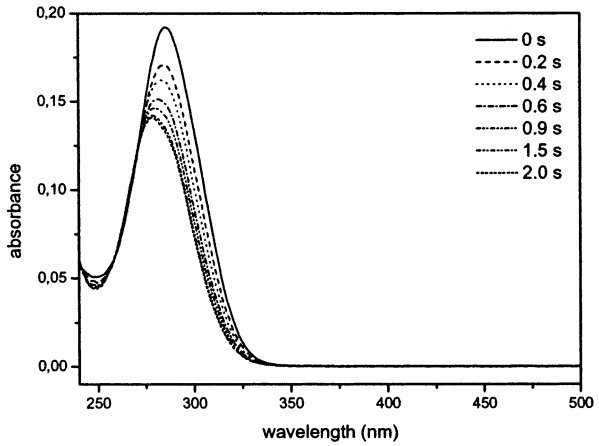

Figure 3. Binding of 5-amino-6-ribitylamino-2,4-(1*H*,3*H*)-pyrimidinedione (compound **2**) to lumazine synthase. Optical spectra from a stopped flow experiment at 25 °C in 100 mM potassium phosphate, pH 6.9. After rapid mixing, the optical cuvette contained 93 μM 5-amino-6-ribitylamino-2,4-(1*H*,3*H*)-pyrimidinedione (compound **2**) and 119 μM enzyme subunits.

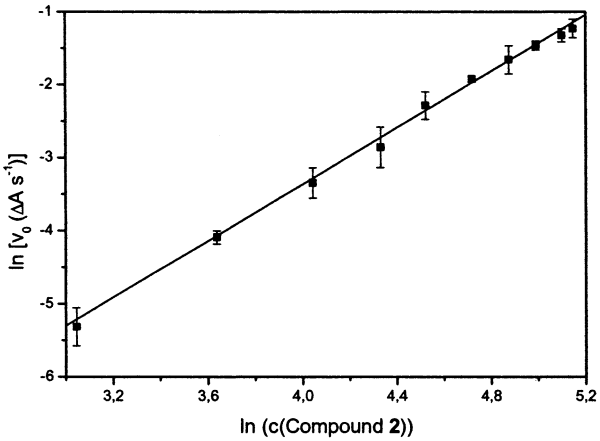

Figure 4. van't Hoff plot of the initial rates (20 °C, 100 mM potassium phosphate, pH 6.9) as a function of the concentration of compound **2**. Experimental points represent the average of four runs with the standard deviation of the mean represented by the vertical bars. Linear regression resulted in a slope of 1.93 ± 0.04 which represents the overall reaction order.

Lumazine synthase binds 6,7-dimethyl-8-ribityllumazine with an apparent K_D of about 160 μM, as shown by equilibrium dialysis experiments. Optical spectra of mixtures containing enzyme and 6,7-dimethyl-8-ribityllumazine at pH 7.0 showed a weak band at about 320 nm, in addition to more intense bands centered at 256, 274, and 408 nm (Figure 2B). 6,7-Dimethyl-8-ribityllumazine without protein displays substantially lower absorption around 320 nm. Binding to the enzyme may increase the acidity; 6,7-dimethyl-8-ribityllumazine absorbance at 320 nm may indicate an anionic, enzyme bound species at neutral pH.

Figure 3 shows optical spectra obtained after rapid mixing of lumazine synthase with the pyrimidine derivative **2**. After rapid mixing, the sample solution contained 93 μM compound **2** and 119 μM lumazine synthase subunits. The dead time was approximately 8 ms, and spectra were acquired at intervals of 100 ms using a diode array detector. We note a decrease of absorbance over a period of about 1 s accompanied by an 8 nm blue shift of the absorbance band of the pyrimidine derivative. The final spectra in Figure 3 agree with the steady-state spectrum of enzyme-bound compound **2** in Figure 2A. Numerical decon-

(26) Pfleiderer, W.; Bunting, J. W.; Perrin, D. D.; Nübel, G. *Chem. Ber.* **1966**, *99*, 3503−3523.
(27) Bown, D. H.; Keller, P. J.; Floss, H. G.; Sedlmaier, H.; Bacher, A. *J. Org. Chem.* **1986**, *51*, 2461−2467.
(28) Beach, R. L.; Plaut, G. W. E. *J. Org. Chem.* **1971**, *36*, 3937−3943.
(29) Bacher, A.; Ludwig, H. C.; Schnepple, H.; Ben Shaul, Y. *J. Mol. Biol.* **1986**, *187*, 75−86.

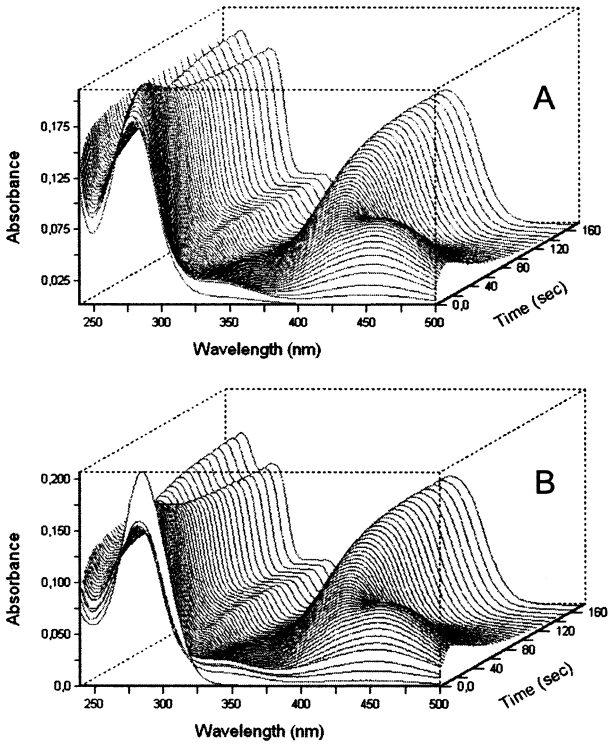

Figure 5. Optical spectra from single turnover stopped flow experiments. (A) Enzyme presaturated with compound **2** was mixed with compound **1**. (B) Enzyme presaturated with compound **1** was mixed with compound **2**. The concentrations after rapid mixing were 97 μM 5-amino-6-ribitylamino-2,4-(1*H*,3*H*)-pyrimidinedione (compound **2**), 383 μM 3,4-dihydroxy-2-butanone 4-phosphate (compound **1**), and 115 μM enzyme subunits.

volution of the spectra using the program SPECFIT/32 indicates a second-order process characterized by a rate constant of 0.017 s^{-1} μM^{-1}.

The overall reaction order of the process was determined by initial rate measurements performed under stopped flow conditions. The reaction scheme in eq 1 affords eq 2 describing a second-order reaction.

$$\text{compound } \mathbf{2} + \text{enzyme} \xrightarrow{k} \text{enzyme}-\text{compound } \mathbf{2} \quad (1)$$

$$-\left(\frac{\mathrm{d}[\text{compound } \mathbf{2}]}{\mathrm{d}t}\right)_{t=0} = v_0 = k[\text{compound } \mathbf{2}]^a[\text{enzyme}]^b \quad (2)$$

When the reactants are used at a stoichiometric ratio of 1:1 (mol of substrate per mol of protein subunits), eq 2 can be rewritten as

$$-\left(\frac{\mathrm{d}[\text{compound } \mathbf{2}]}{\mathrm{d}t}\right)_{t=0} = v_0 = k_{(a+b)}[\text{compound } \mathbf{2}]^{(a+b)} \quad (3)$$

In logarithmic form, eq 3 can be rewritten as

$$\ln(v_0) = (a + b)\ln(\text{compound } \mathbf{2})_0 + \ln(k_{(a+b)}) \quad (4)$$

As shown in Figure 4, a van't Hoff plot of the initial rates of ligand binding afforded a straight line with a slope of 1.93. Thus, ligand binding must be described as a second-order process. Calculation of k_{on} using the intercept of the *y*-axis ($-11.1 \pm$

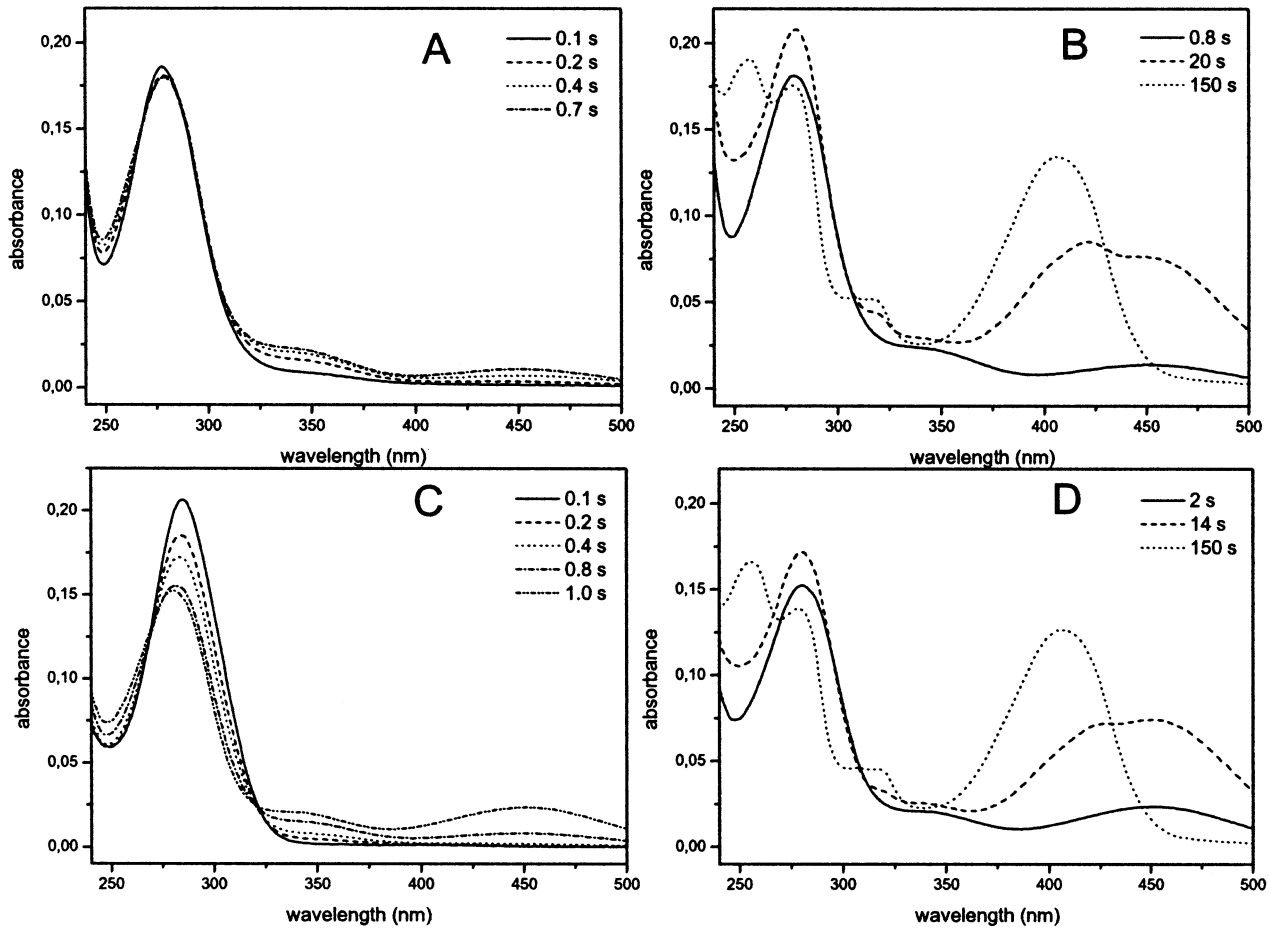

Figure 6. Ultraviolet spectra from the early phase (A, C) and the later phase (B, D) of the single turnover experiments shown in Figure 5.

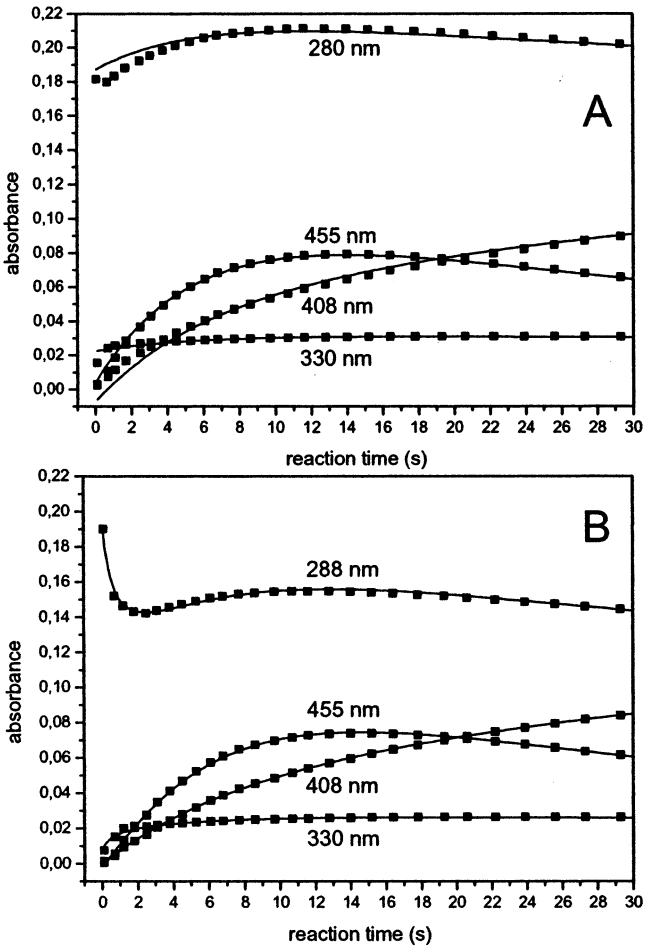

Figure 7. Absorbance changes observed during the single turnover stopped flow experiments shown in Figure 6. Symbols represent experimental data from Figure 6. Solid lines represent the numerical simulation using the kinetic constants in Table 1. For other details, see legend to Figure 6.

0.2; ϵ for compound **2** at 284 nm = 15 000 M^{-1} cm^{-1}; path length, 1.5 mm) results in a value of 0.0067 μM^{-1} s^{-1} at 20 °C. With an apparent K_D of about 9 μM, k_{off} can be calculated as 0.06 s^{-1}.

Stopped flow experiments involving both enzyme substrates (i.e., compounds **1** and **2**) are shown in Figures 5−8. In these experiments, 3,4-dihydroxy-2-butanone 4-phosphate **1** was proffered at a 3.3-fold excess over the concentration of enzyme subunits in order to ensure saturation of the enzyme and to minimize problems involved in the kinetic analysis of a two-substrate reaction. This could be done without compromising the optical measurements, since the carbohydrate phosphate is transparent in the spectral range of the stopped flow experiment.

The experiment in Figure 5A involved the rapid mixing of compound **1** with a mixture containing compound **2** and lumazine synthase subunits. After rapid mixing, the solution contained 115 μM enzyme subunits, 383 μM compound **1**, and 97 μM compound **2**. Optical spectra were then acquired at intervals of 100 ms over a spectral range of 240−500 nm. Selected spectra are replotted for clarity in Figure 6A,B. Absorption at selected wavelengths as a function of reaction time is shown in Figure 7A.

The initial reaction phase is characterized by the rapid appearance of a very low intensity absorption band with a maximum at about 330 nm (Figure 6A). The subsequent reaction phase is dominated by absorbance in the long wavelength range with maxima around 455 and 408 nm. The absorbance above 450 nm reaches a maximum value at 17 s and subsequently decreases to low values over a period of about 2 min.

Absorbance at 408 nm, the λ_{max} of the enzyme product **8** begins to increase from a very low value at approximately 1 s after mixing and reaches a plateau after about 120 s. At the end of the single turnover reaction, the optical spectrum of the reaction mixture is similar to that of a steady state mixture of enzyme and 6,7-dimethyl-8-ribityllumazine, as shown in Figure 2B. The maxima at 406, 280, and 255 nm clearly represent the neutral form of 6,7-dimethyl-8-ribityllumazine. The additional maxima at 307 and 317 nm may represent a protein-bound anion form of 6,7-dimethyl-8-ribityllumazine.

In a similar experiment, a solution containing compound **2** was rapidly mixed with a solution containing compound **1** and protein (Figure 5B). The final concentrations in the optical cuvette were identical with to those in Figure 5A (115 μM enzyme subunits, 383 μM compound **1**, and 97 μM compound **2**), although they were obtained by a different mixing protocol. In excellent agreement with expectations based in the foregoing experiments, Figures 5B, 6C and D, 7B, and 8C and D show a rapid decrease at 284 nm in close similarity with the experiment in Figure 2A (notably, that rapid decrease of absorbance is not observed in Figure 5A where the reaction mixture was obtained by a different mixing protocol). Later, Figure 7A shows a rapid appearance of the low absorbance transient at 330 nm which is observed earlier in Figure 6A. The spectra obtained in the late reaction phase (later than 5 s) are closely similar in Figure 5A and B; the optical spectra in Figure 6B and D become fairly similar.

Numerical deconvolution of the data in Figure 5A indicated two linearly independent processes (Figure 8A,B). A transient species with absorbance at 455 and 282 nm reached a maximum concentration at about 17 s and was subsequently consumed under formation of 6,7-dimethyl-8-ribityllumazine. This reactionsequence can be described by the following equation:

$$A \xrightarrow{k_2} C \xrightarrow{k_3} D \qquad (5)$$

The numerical deconvolution failed to pick up the weak and early optical transient characterized by an absorption of 330 nm. This failure is not surprising in light of (i) the weak absorbance of the transient species and (ii) the rapid appearance of absorbance contribution by the transient species B and of 6,7-dimethyl-8-ribityllumazine in the enzyme bound anionic form.

A similar deconvolution analysis of the experiment in Figure 5B is shown in Figure 8C,D. The analysis supports three linearly independent processes. This reaction sequence can be described by the following equation:

$$A \xrightarrow{k_1[2]} B \xrightarrow{k_2} C \xrightarrow{k_3} D \qquad (6)$$

The first optical transient virtually duplicates the second-order process observed in Figure 3 (mixing of enzyme with compound **2**). The apparent rate constant k_1 is 0.017 s^{-1} μM^{-1}, in close similarity with the rate constant for the experiment in Figure 3.

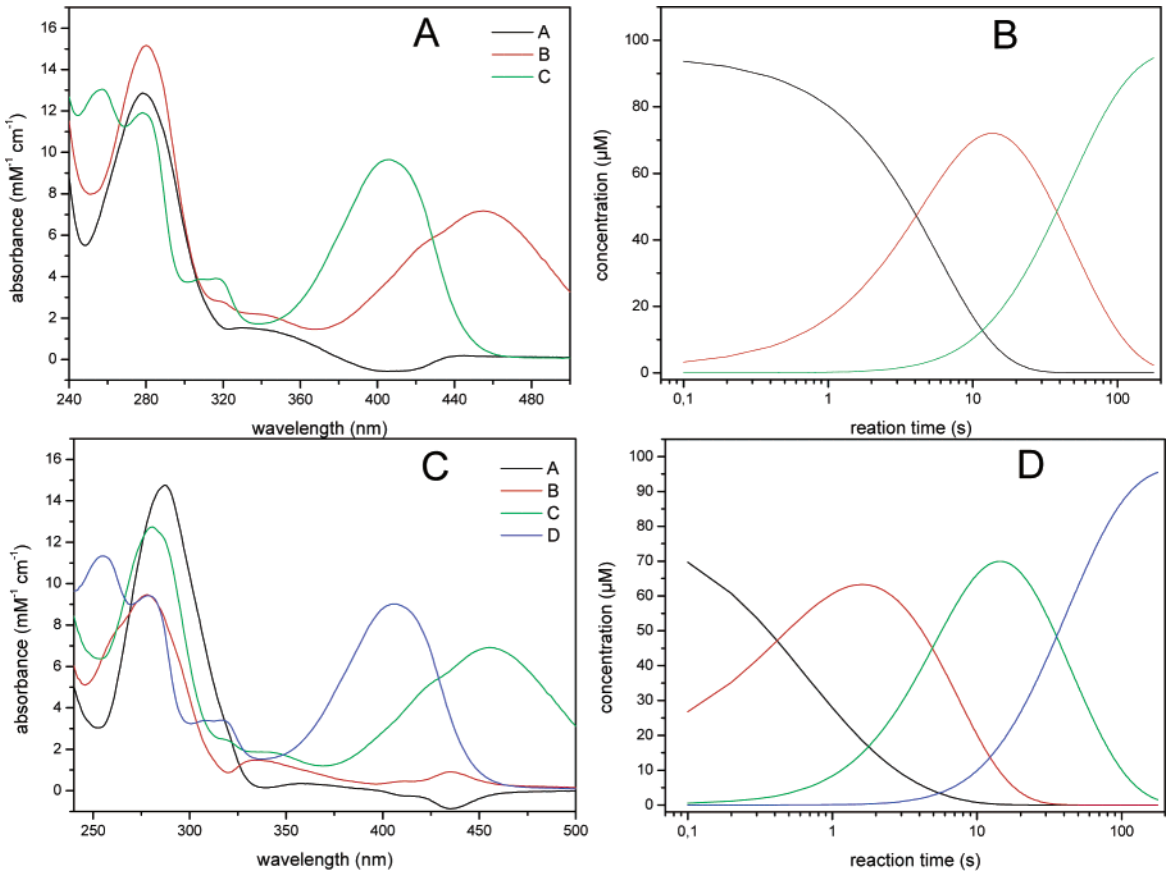

Figure 8. Numerical deconvolution of the stopped flow data shown in Figure 5. (A, C) Reconstructed absorbance spectra of transient chromophors. (B, D) Concentration of transient species.

The numerical values for k_2 and k_3 are closely similar in the experiments shown in Figure 5A and B.

Discussion

Binding of compound **2** to lumazine synthase proceeds as a second-order reaction with a rate around 0.02 s^{-1} μM^{-1} as shown by initial rate measurements under stopped flow conditions (Figure 4). Thus, k_{on} is low by comparison with those of most enzymes, but the same holds true for the overall catalytic rate of lumazine synthase.

The rate constant for binding of the substrate **2** is not significantly affected by the presence or absence of the second substrate. Hence, the loading of the enzyme with the substrates **1** and **2** lacks the characteristics of an ordered process.

The low k_{on} rate of lumazine synthase may be related to the unusual structure of the protein. The catalytic sites are located close to the inner surface of the icosahedral capsid.[12,30] The equilibrium X-ray structure fails to explain how substrates and products penetrate the densely packed capsids wall, and major dynamic motions of the capsid structure have been proposed as a possible mode for substrate and product exchange with the bulk solvent. A low rate for the penetration of substrate and products through the capsid wall is well in line with the observation of intermediate channeling in the enzyme complex comprising an icosahedral lumazine synthase capsid with a core of riboflavin synthase (heavy riboflavin synthase).[12,16]

The early transient absorbing weakly around 330 nm can be attributed tentatively to the Schiff base intermediate **3** in Figure 1. The π electron system of the hypothetical Schiff base intermediate **3** is similar to that of dihydropterins such as dihydroneopterin with absorbance maxima at 330 nm ($\epsilon = 6300$ M^{-1} cm^{-1}) and 280 nm.[31]

The transient C with an absorption maximum at 455 nm suggests an extended π electron system. The hypothetical intermediates **4**, **5**, and **6** have extended π electron systems which appear sufficient for the observed long wavelength absorption, but an unequivocal structural assignment of the 455 nm transient is not yet possible.

Stopped flow experiments with lumazine synthase of *Magnaporthe grisea* have been reported by Zheng et al.[32] The authors used single wavelength detection at 408 nm and interpreted the absorbance at that wavelength as a measure for product formation. This interpretation ignores the absorbance contribution of the optical transient C with an absorption maximum at 455 nm which has a significant absorbance at 408 nm ($\epsilon_{455}/\epsilon_{408} = 0.5$). Due to the failure to detect that highly absorbing species, the kinetic model of Zheng et. al. is bound to become incorrect.

The rate-limiting step in our experiments is the formation of 6,7-dimethyl-8-ribityllumazine **8** but cannot be unequivocally

(30) Ladenstein, R.; Meyer, B.; Huber, R.; Labischinski, H.; Bartels, K.; Bartunik, H. D.; Bachmann, L.; Ludwig, H. C.; Bacher, A. *J. Mol. Biol.* **1986**, *187*, 87−100.

(31) Pfleiderer, W. In *Folates and Pterins*; Blakely, R. L., Benkovic, S. J., Eds.; John Wiley & Son: New York, 1985; Vol. 2, pp 43−114.

(32) Zheng, Y.-J.; Viitanen, P. V.; Jordan, D. B. *Bioorg. Chem.* **2000**, *28*, 89−97.

Table 1. Kinetic Constants Obtained from Single Turnover Stopped Flow Experiments with Recombinant Lumazine Synthase from *B. subtilis*[a]

experiment	1	2	3
k_1 (s^{-1} μM^{-1})	0.020 ± 0.0007		0.017 ± 0.01
k_2 (s^{-1})		0.17 ± 0.001	0.18 ± 0.003
k_3 (s^{-1})		0.022 ± 0.0002	0.024 ± 0.0002

[a] Experiment 1, enzyme mixed with compound **2** without the second substrate compound **1**; experiment 2, enzyme preincubated with compound **2** and mixed with compound **1**; experiment 3, enzyme preincubated with 3,4-dihydroxy-2-butanone 4-phosphate (compound **1**) and mixed with 5-amino-6-ribitylamino-2,4-(1*H*,3*H*)-pyrimidinedione (compound **2**).

attributed to a specific reaction step in Figure 1, since the 455 nm transient may represent any of the hypothetical intermediates **4**−**6**. More specifically, the rate constant k_3 (Table 1) may comprise any of the following reactions: (i) the enolization of **5**, (ii) the rotation of the position 5 side chain from the extended conformation observed in the crystallographic studies with the intermediate analogue 5-(6-D-ribitylamino-2,4-dihydroxypyrimidine-5-yl)-1-pentenyl phosphonic acid into a conformation where the position 8 amino group can attack the carbonyl group of the position 7 side chain, (iii) the ring closure reaction, and (iv) the elimination of water from the covalent hydrate **7**.

Oschkinat et al.[33] studied the conformation of 6,7-dimethyl-8-ribityllumazine bound to lumazine synthase by transfer NOE NMR experiments. The observation of transfer NOE cross peaks between the signals of the free and the enzyme bound ligand requires that the dissociation of the enzyme product complex occurs on the time scale of the NMR experiment. Although k_{off} for the bound product has not been measured, the dissociation of the complex as observed qualitatively by NMR is definitely too rapid to come even close to being the rate-limiting step of the overall enzyme reaction, as suggested by Zheng et al.[32]

The detailed kinetic analysis of complex enzyme mechanisms by time-resolved optical spectroscopy is only possible if at least certain reaction components have characteristic spectra in the visible and/or near-ultraviolet range. Certain enzymes involved in the biosynthesis of bicyclic heterocycles such as GTP cyclohydrolase I catalyzing the formation of dihydroneopterin triphosphate and lumazine synthase are particularly favorable for that type of analysis due to the sequence of "colorful" reaction intermediates and their relatively low reaction rates.[34,35]

Acknowledgment. This work was supported by the Deutsche Forschungsgemeinschaft, by European Community Grant ERB FMRX CT98-0204, the Fonds der Chemischen Industrie, and the Hans Fischer-Gesellschaft.

JA028226K

(33) Oschkinat, H.; Schott, K.; Bacher, A. *J. Biomol. NMR* **1992**, *2*, 19−32.
(34) Schramek, N.; Bracher, A.; Fischer, M.; Auerbach, G.; Nar, H.; Huber, R.; Bacher, A. *J. Mol. Biol.* **2001**, *316*, 827−835.
(35) Bracher, A.; Schramek, N.; Bacher, A. *Biochemistry* **2001**, *40*, 7896−7902.